Genotoxicity assessment of magnetic iron oxide nanoparticles with different particle sizes and surface coatings

2014 Nanotechnology 25 425101

(http://iopscience.iop.org/0957-4484/25/42/425101)

IOP Publishing Nanotechnology
Nanotechnology **25** (2014) 425101 (11pp) doi:10.1088/0957-4484/25/42/425101

Genotoxicity assessment of magnetic iron oxide nanoparticles with different particle sizes and surface coatings

Yanping Liu[1], Qiyue Xia[1], Ying Liu[1], Shuyang Zhang[1], Feng Cheng[1], Zhihui Zhong[2], Li Wang[1], Hongxia Li[1] and Kai Xiao[1,2]

[1] National Chengdu Center for Safety Evaluation of Drugs, State Key Lab of Biotherapy, West China Hospital, Sichuan University, Chengdu 610041, People's Republic of China
[2] Laboratory of Non-Human Primate Disease Model research, State Key Lab of Biotherapy, West China Hospital, Sichuan University, Chengdu 610041, People's Republic of China

E-mail: iamxiaokai@hotmail.com and hxl9998@sohu.com

Received 10 July 2014, revised 25 August 2014
Accepted for publication 29 August 2014
Published 2 October 2014

Abstract

Magnetic iron oxide nanoparticles (IONPs) have been widely used for various biomedical applications such as magnetic resonance imaging and drug delivery. However, their potential toxic effects, including genotoxicity, need to be thoroughly understood. In the present study, the genotoxicity of IONPs with different particle sizes (10, 30 nm) and surface coatings (PEG, PEI) were assessed using three standard genotoxicity assays, the *Salmonella typhimurium* reverse mutation assay (Ames test), the *in vitro* mammalian chromosome aberration test, and the *in vivo* micronucleus assay. In the Ames test, SMG-10 (PEG coating, 10 nm) showed a positive mutagenic response in all the five test bacterial strains with and without metabolic activation, whereas SEI-10 (PEI coating, 10 nm) showed no mutagenesis in all tester strains regardless of metabolic activation. SMG-30 (PEG coating, 30 nm) was not mutagenic in the absence of metabolic activation, and became mutagenic in the presence of metabolic activation. In the chromosomal aberration test, no increase in the incidence of chromosomal aberrations was observed for all three IONPs. In the *in vivo* micronucleus test, there was no evidence of increased micronuclei frequencies for all three IONPs, indicating that they were not clastogenic *in vivo*. Taken together, our results demonstrated that IONPs with PEG coating exhibited mutagenic activity without chromosomal and clastogenic abnormalities, and smaller IONPs (SMG-10) had stronger mutagenic potential than larger ones (SMG-30); whereas, IONPs with SEI coating (SEI-10) were not genotoxic in all three standard genotoxicity assays. This suggests that the mutagenicity of IONPs depends on their particle size and surface coating.

Keywords: iron oxide nanoparticles, particle size, surface coating, genotoxicity, bacterial reverse mutation test, chromosome aberration test, micronucleus test

1. Introduction

In recent years, magnetic iron oxide nanoparticles (IONPs) have attracted much attention not only because of their superparamagnetic properties but also because they hold great potential in many biomedical applications such as drug delivery, magnetic resonance imaging (MRI) contrast enhancement, and in the targeted destruction of tumor tissue through hyperthermia [1]. The increasing applications of magnetic IONPs, have given rise to many concerns among public, scientific and regulatory authorities regarding their safety and final fate in biological systems. Although information about the toxicity of IONPs continues to increase, a significant knowledge gap exists on a complete toxicological profile of these promising nanoparticles proposed for safe future use in many aspects of biomedical engineering. There have been some studies on the toxicity of nanoparticles [2–4], however, they have primarily focused on the cytotoxicity of

nanoparticles and thus the genotoxicity evaluation has largely been overlooked. In addition, few studies concern the oral, especially intravenous routes of administration, which are more relevant for most nanoparticles of interest in nanomedicine [5].

Only a few papers regarding the genotoxicity of IONPs have been reported so far, and even the results among them are controversial. For example, Sadiq *et al* [6] reported that no cytotoxic and genotoxic effects were observed for IONPs in commonly used genotoxicity assays, including Ames assay, micronucleus assay and comet assay. On the contrary, another report showed that IONPs had mutagenic activity without chromosomal abnormalities at the concentration of 70 ppm [2]. It is possible that the inconsistency in the literature is due to different types of IONPs tested, the study design and/or inadequate characterization of the physico-chemical properties (such as particle size, shape, and surface coating) of the nanomaterials [7]. Experience with non-nano substances taught us that the mechanisms of genotoxic effects could be diverse. Therefore, evaluation of the potential genotoxicity of nanomaterials should include a set of genotoxicity assay with different genotoxicity endpoints to cover as many potential forms of DNA damage that may be induced following exposure to nanoparticles [2].

With regards to cellular uptake, there are several different mechanisms by which nanomaterials can be internalized, perhaps the most prominent being diffusion across the plasma membrane (either directly across the membrane or through membrane channels (10–30 nm wide)) or by endocytosis, an energy dependent mechanism that can involve a number of different routes [1]. The physico-chemical characteristics of nanoparticles such as composition, particle size, surface charge and surface hydrophobicity may affect their interaction with plasma proteins (opsonins) and blood components (hematocompatibility), cellular uptake pathways and intracellular fates, hence potentially influence their *in vivo* fate, targeted delivery, and toxicity [8]. Xiao *et al* [9] systematically elucidate the effect of surface charge on the cellular uptake and *in vivo* fate of PEG-oligocholic acid based micellar nanoparticles, and they found that the physico-chemical characteristics of nanoparticles such as surface charge had tremendous impacts on their pharmacokinetic and pharmacodynamic profiles such as biodistribution, elimination and tumor targeting property. However, the effect of physico-chemical properties such as particle size and surface coating on the genotoxicity of nanoparticles is poorly understood.

The aim of this study is to test the hypothesis that the genotoxicity of nanoparticles including IONPs can be modulated by their physico-chemical characteristics such as size and coating. IONPs with different surface coating (poly (ethylene glycol), PEG, neutral; poly(ethylene imine), PEI, positively charged), and different particle size (10 nm, 30 nm) were chosen for the genotoxicity evaluation, using a battery of standardized tests, including the *Salmonella typhimurium* reverse mutation assay (Ames test), the *in vitro* mammalian chromosome aberration test, and the *in vivo* micronucleus assay. We believe that this study will help to improve our understanding of the genotoxicity and the underlying mechanisms of IONPs.

2. Materials and methods

2.1. IONPs

IONPs with neutral non-functional PEG coating and different particle size (10 nm, SMG-10; 30 nm, SMG-30), and IONPs with positively charged PEI surface (10 nm, SEI-10) were obtained from Ocean NanoTech, LLC. Their characteristics as reported by the manufacturer are: SEI-10, solution in DI water, 5–10 pH stability, 1 mg ml^{-1} (Fe); SMG-10 and SMG-30, solution in Borate (0.01 M, pH 5.0), 5–10 pH stability, 1 mg ml^{-1} (Fe).

The morphology and particle size of IONPs were observed on a Philips CM-120 transmission electron microscope (TEM) operating at an acceleration voltage of 80 kV. IONPs were homogeneously dispersed in water, and one drop of the suspension was deposited on a TEM grid, dried, and evacuated before analysis. The particle size distribution and zeta potential of IONPs were measured by dynamic light scattering (DLS) using Zetatrac (Microtrac) as described previously [10].

2.2. Sample preparation

The SMG-10, SMG-30 and SEI-10 were aqueous solution. In each experiment, they were diluted in sterile physiological saline.

2.3. Preparation of mammalian liver S9 fraction

The S9 fraction was prepared from the livers of male Sprague–Dawley rats treated with the combination of phenobarbital/β-naphthoflavone according to the method described by Elliot *et al* [11]. The S9 metabolic activator was prepared immediately before use, by adding: 0.1 ml of S9 fraction and 0.9 ml of cofactor. Thus, 1 ml of S9 mix contained 0.1 ml S9 (10%), 0.2 M of phosphate buffer (pH 7.4), 8 μM of $MgCl_2$, 33 μM of KCl, 5 μM of glucose-6-phosphate, and 4 μM of NADP. The S9 mixture was kept on ice during testing.

2.4. Ames test

The experiments were conducted according to the OECD Guideline for Testing of Chemicals 471 'Bacterial Reverse Mutation Test' [12]. *S. typhimurium* TA98 (hisG3052 rfa ΔuvrB pKM101), *S. typhimurium* TA100 (hisG46 rfa ΔuvrB pKM101), *S. Typhimurium* TA1535 (hisG46 rfa ΔuvrB), *S. typhimurium* TA97 (hisD6610 rfa ΔuvrB pKM101) and *S. Typhimurium* TA102 (hisG428 rfa pKM101 pAQ1), were supplied by *Molecular Toxicology*. The strain genotypes were confirmed by testing the presence of specific genetic markers and phenotypes in preliminary strain check assays. The tester strains used in each experiment were freshly prepared by preculturing them into the nutrient broth after incubation overnight (13–16 h) at 37 °C.

Top agar was prepared by dissolving 6 g of agar (Kelong Chemical, Chengdu, China) and 5 g of NaCl in 1000 ml of purified water and sterilizing the solution for 10–15 min at 121 °C using an autoclave. For the culture of *S. typhimurium*, a mixed aqueous solution of L-Hsitidine (0.5 mM) and D-biotin (0.5 mM) was added to the agar medium.

Plate incorporation assay was applied to detect reverse mutation in the presence and absence of metabolic activation, using an S9 mix [13]. For the direct method (no metabolic activation), 0.5 ml of purified water and 0.1 ml of each bacterial suspension were added to top agar (2 ml, maintained at 55 °C) with physiological saline, SEI-10, SMG-10, SMG-30, or the positive controls (100 μl each). For the metabolic activation method, 0.5 ml of the S9 mix and 0.1 ml of each bacterial suspension were added to top agar (2 ml, maintained at 55 °C) with physiological saline, SEI-10, SMG-10, SMG-30 or the positive controls (100 μl each). The mixtures were poured into plates and incubated at 37 °C for 48 h. The number of revertant colonies was counted using an automatic colony counter (Hangzhou Shineso Science & Technology, China).

The maximum concentration of test substances were 1 mg ml^{-1}, the volume of administration was 100 μl of test substances per plate; hence, the highest dose corresponded to 100 μg per plate. Based on our preliminary data, 100 μg per plate was set as the highest concentration for SEI-10 with and without S9; 20 μg per plate was set as the highest concentration with S9 and 100 μg per plate without S9 for SMG-30; and 20 μg per plate was set as the highest concentration for SMG-10 with and without S9. Five-fold intervals were set for the descending dose levels.

The toxicity of the test materials was evaluated as reduction in the number of revertant colonies and as change in the auxotrophic background growth (background lawn) in comparison with control plates [14]. A positive response in the test was defined as an increase (at least two-fold above the control) in histidine independent revertant colonies in every strain with a dose- response relationship [15].

2.5. In vitro mammalian chromosome aberration test

The experiments were conducted according to the OECD Guideline for Testing of Chemicals 473, '*In vitro* Mammalian Chromosomal Aberration Test' [16]. Chinese hamster lung (CHL) cells were obtained from Shanghai Institutes for Biological Sciences (Shanghai, China). The CHL cells were cultured in MEM medium (Hyclone) containing 10% (v/v) heat-inactivated Calf serum, 100 U ml^{-1} penicillin and 100 μg ml^{-1} streptomycin at 37 °C in a humidified 5% CO_2 incubator, and passaged once every 2–3 days. Serum was obtained from GIBCO and antibiotics were from North China Pharmaceutical Group Corporation. The vehicle control used was physiological saline. The positive control substances used were 0.25 μg ml^{-1} mitomycin C (MMC) for the exposure without metabolic activation, and 25 μg ml^{-1} cyclophosphamide (CPA) for the exposure with metabolic activation, respectively.

The test was performed in the presence and absence of metabolic activation (S9 mix). The final concentration of S9 in the treatment medium was 10% (v/v). The study consisted of short-term exposure (4 h, with and without metabolic activation) and continuous exposure (24 h, without metabolic activation). In both cases, about 5×10^4 cells were seeded on each tissue culture flasks (50 ml) and incubated at 37 °C in 5 ml of culture medium for 24–48 h. For short-term exposure, the test substances were administrated for 4 h followed by a recovery period of 20 h. For the metabolic activation, the cells were treated with the S9 mix (0.5 ml) together with the test substances (0.1 ml). For continuous exposure, the test substances were kept in culture for 24 h. All the cells were sampled at 24 h after the beginning of treatment. At 4 h before sampling, they were treated with colchicine (Sigma; 0.4 μg ml^{-1} final concentration), harvested, stained and metaphase cells were analyzed microscopically for the presence of chromosome aberrations. Two hundred metaphases per dose were examined for structural aberrations and polyploidy. A cell growth inhibition test was also concomitantly conducted under the same conditions.

The maximum concentration of test substances were 1 mg ml^{-1}, the volume of administration was 0.1 ml of test substances into 4.9 ml of culture medium; hence, the highest dose corresponded to 20 μg ml^{-1}. In the preliminary test, SMG-10 and SMG-30 administered at the maximum final concentration of 20 μg ml^{-1} did not have any cytotoxicity, whereas SEI-10 caused cell growth inhibition at the concentration of 10 μg ml^{-1}. In the presence of cytotoxicity, the top concentration selected should be one that caused 50% or greater inhibition of cell growth compared to the negative control. According to the results of the preliminary test, the concentrations of SEI-10 selected for the main test were 0.94, 1.88, 3.75, 7.5 and 15 μg ml^{-1} for the short exposure; 0.63, 1.25, 2.5, 5 and 10 μg ml^{-1} selected for continuous exposure. The concentrations of SMG-10 and SMG-30 selected for the main test were 2.5, 5, 10, 20 μg ml^{-1} for the short and continuous exposure. Duplicate plates were examined at each dose.

The clastogenic potential was judged as negative, suspicious and positive if the incidence of cells showing any aberrations was <5%, 5%–10% and >10%, respectively [17].

2.6. In vivo mammalian erythrocyte micronucleus test

The experiments were conducted according to the OECD Guideline for Testing of Chemicals 474 'Mammalian Erythrocyte Micronucleus Test' [18]. Adult male NIH mice (5–6 weeks old, 25–30 g body weight) obtained from the breeding center of Guangdong Medical Laboratory Animal were used. The mice were housed in clean polypropylene cages and maintained in an air-conditioned conventional animal house at 23 ± 3 °C, 40%–70% relative humidity and 12 h light/dark cycle (light on at 07:30). The animals were provided with commercial rat pellet (Shanghai SLAC Laboratory Animal) and tap water *ad libitum.*

After 5 days acclimatization, the mice were randomly assigned to the control and treatment groups ($n = 6$): negative

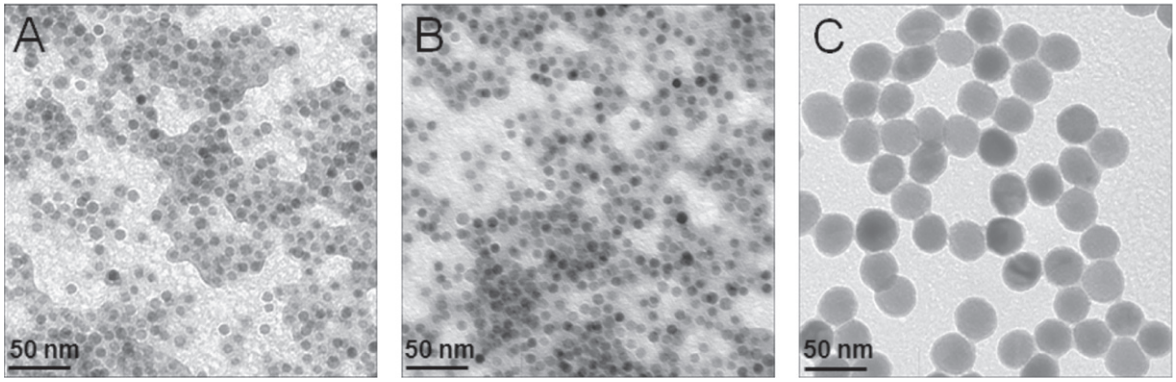

Figure 1. Representative TEM images of SEM-10 (A), SMG-10 (B) and SMG-30 (C). IONPs were deposited on copper coated grids and dried for TEM imaging. Images were analyzed in high resolution mode with an acceleration voltage of 80 kV.

control (physiological saline), positive control (CPA, 40 mg kg^{-1}), SEI-10, SMG-10 and SMG-30 (low, medium, and high dose). Animals were administered with negative control (physiological saline), SEI-10, SMG-10 and SMG-30 via intravenous injection, once daily for 4 consecutive days, respectively; and animals in the positive control group were administered with CPA (40 mg kg^{-1}) via intraperitoneal injection once at the 4th day. The injected volume was 10 ml kg^{-1} body weight. After dosing, the mice were examined regularly for mortality and clinical signs of toxicity until they were euthanized. The femurs of mice in all groups were removed 24 h after the final administration, and the bone marrow cells were collected with calf serum to prepare bone marrow smear specimens. The specimens were air-dried, fixed with methanol and stained with Giemsa (1 ml of the dye was diluted ten-fold with phosphate buffer) for about 20 min at room temperature. The animals received humane care and the study protocol was approved by Institutional Animal Care and Use Committee of National Chengdu Center for Safety Evaluation of Drugs, West China Hospital, Sichuan University.

A preliminary test was carried out for maximal tolerance in two male via intravenous injection once daily per day for four days. The maximum concentrations of test substances were 1 mg ml^{-1}. The volume of administration was 10 ml kg^{-1}; hence, the highest dose corresponded to 10 mg kg^{-1}. No death was found and no abnormalities were detected in mice treated with SMG-10 and SMG-30 at doses of 2.5–10 mg kg^{-1}. However, SEI-10 caused animal death at 2.5 mg kg^{-1} or higher doses. Therefore, in the *in vivo* micronucleus test, the doses set for SMG-10 and SMG-30 were 2.5 mg kg^{-1}, 5 mg kg^{-1} and 10 mg kg^{-1}, respectively; and the doses set for SEI-10 were 0.38 mg kg^{-1}, 0.75 mg kg^{-1} and 1.5 mg kg^{-1}, respectively.

The frequency of micronucleated polychromatic erythrocytes (MNPCE) was calculated on the basis of observations of 2000 polychromatic erythrocytes (PCE) per animal. Furthermore, the proportion of PCE among total erythrocytes (TE) was determined by counting 200 erythrocytes for each mouse. The result was judged positive if a statistically significant increase in the frequency of MNPCE was observed at least one dose level of SEI-10, SMG-10 or SMG-30, accompanied by a dose-response relationship.

2.7. Statistical analysis

All values were expressed as mean ± SD in Ames test and micronucleus test. Results were tested for significance with one-way analysis of variance (ANOVA). The percentage of cells with aberrations was presented with contingency table and evaluated using Fisher exact probability test (EXACT). A value of $P < 0.05$ was considered statistically significant.

3. Results

3.1. Physical characterization of IONPs

TEM images (figure 1) demonstrated that all three IONPs were spherical, and homogeneous in size. The particle sizes of both SEI-10 and SMG-10 were around 10 ~ 20 nm in diameter, and the particle size of SMG-30 was around 30 ~ 40 nm in diameter. DLS measurement indicated that the average size of SEI-10, SMG-10, and SMG-30 were 17 ± 5 nm, 16 ± 5 nm, and 36 ± 16 nm, respectively, which were consistent with the observation under TEM. The zeta potential (surface charge) of SEI-10, SMG-10, and SMG-30 in water were +29.3 mV, −0.5 mV, and −0.5 mV, respectively.

3.2. Ames test

Table 1 (without S9) and table 2 (with S9) show the results of the main test of *in vitro* reverse mutation. Positive controls induced increases in the number of revertant colonies, confirming the sensitivity of the test system. There was no growth inhibition at any concentration of SMG-10, SMG-30 and SEI-10 with and without metabolic activation.

The number of revertant colonies for SMG-10 without metabolic activation significantly increased at 0.8–20.0 μg per plate in TA97, 4.0–20.0 μg per plate in TA98 and TA100, 20.0 μg per plate in TA102 and 0.16–20.0 μg per plate in TA1535, when compared to the spontaneous reversion rate in the negative control ($P < 0.05$). In the presence of metabolic

Table 1. Mutagenicity of IONPs in *Salmonella typhimurium* tester strains without metabolic activation (–S9).

Group	Concentration (μg per plate)	Number of revertant colonies per plate (mean ± SD)				
		TA97	TA98	TA100	TA102	TA1535
Negative	0	64 ± 18	16 ± 1	159 ± 20	203 ± 28	17 ± 4
Positive[a]		478 ± 92[b]	434 ± 13[b]	1117 ± 317[b]	2000 ± 113[b]	352 ± 80[b]
SEI-10	0.16	43 ± 12	27 ± 4[b]	161 ± 8	203 ± 42	18 ± 3
	0.8	51 ± 7	18 ± 2	143 ± 5	199 ± 14	24 ± 6
	4.0	44 ± 27	19 ± 5	147 ± 28	160 ± 79	24 ± 9
	20.0	56 ± 27	20 ± 5	150 ± 21	215 ± 39	23 ± 6
	100.0	63 ± 22	16 ± 2	124 ± 58	138 ± 32	26 ± 11
SMG-10	0.032	123 ± 21[b]	13 ± 5	154 ± 8	256 ± 69	19 ± 8
	0.16	79 ± 40	20 ± 6	138 ± 15	250 ± 78	55 ± 24[b]
	0.8	144 ± 19[b]	17 ± 2	160 ± 16	293 ± 51	109 ± 77[b]
	4.0	136 ± 74[b]	59 ± 29[b]	500 ± 84[b]	330 ± 149	612 ± 222[b]
	20.0	723 ± 251[b]	161 ± 53[b]	920 ± 259[b]	630 ± 156[b]	1014 ± 257[b]
SMG-30	0.032	91 ± 38	12 ± 6	162 ± 18	207 ± 35	41 ± 18
	0.16	101 ± 13	19 ± 5	162 ± 33	161 ± 29	37 ± 17
	0.8	99 ± 74	13 ± 1	132 ± 17	188 ± 38	33 ± 6
	4.0	73 ± 21	16 ± 4	153 ± 25	230 ± 54	37 ± 7
	20.0	112 ± 42	12 ± 5	159 ± 7	204 ± 70	33 ± 6
	100	76 ± 6	20 ± 6	140 ± 15	225 ± 35	24 ± 8

[a] Positive controls were sodium azide (1.5 μg per plate, Sigma) for TA1535 and TA100 strains, 2,4,7-trinitro-9-fluorenone (0.2 μg per plate, Kaoensi Science&Technology, Chengdu, China) for TA98 and TA97 strains, mitomycin C (MMC; 0.5 μg per plate, Wako Pure Chemial) for the TA102 strain, respectively.
[b] $P < 0.05$, when compared to negative control.

Table 2. Mutagenicity of IONPs in *Salmonella typhimurium* tester strains with metabolic activation (+S9).

Group	Concentration (μg per plate)	Number of revertant colonies per plate (mean ± SD)				
		TA97	TA98	TA100	TA102	TA1535
Negative	0	38 ± 26	20 ± 15	126 ± 14	246 ± 17	19 ± 10
Positive[a]		782 ± 112[b]	1370 ± 186[b]	655 ± 199[b]	846 ± 60[b]	219 ± 95[b]
SEI-10	0.16	22 ± 22	15 ± 6	83 ± 5[b]	220 ± 69	19 ± 7
	0.8	19 ± 17	12 ± 6	89 ± 12[b]	185 ± 33	12 ± 2
	4.0	29 ± 10	22 ± 8	78 ± 9[b]	207 ± 64	11 ± 1
	20.0	24 ± 8	14 ± 1	102 ± 11	255 ± 31	8 ± 3
	100.0	60 ± 6	16 ± 3	97 ± 12[b]	180 ± 13	10 ± 3
SMG-10	0.032	150 ± 20[b]	53 ± 6[b]	120 ± 17	250 ± 3	36 ± 7
	0.16	262 ± 57[b]	198 ± 65[b]	161 ± 16	332 ± 86	188 ± 23[b]
	0.8	457 ± 200[b]	656 ± 234[b]	105 ± 15	202 ± 19[b]	428 ± 43[b]
	4.0	612 ± 109[b]	617 ± 109[b]	676 ± 67[b]	567 ± 74[b]	615 ± 50[b]
	20.0	1767 ± 93[b]	1854 ± 237[b]	1158 ± 74[b]	1371 ± 155[b]	1756 ± 76[b]
SMG-30	0.032	91 ± 7	34 ± 7	222 ± 67[b]	216 ± 16	14 ± 5
	0.16	108 ± 26[b]	43 ± 12[b]	246 ± 31[b]	249 ± 11	21 ± 4
	0.8	111 ± 17[b]	25 ± 11	219 ± 17[b]	214 ± 45	24 ± 5
	4.0	107 ± 19[b]	171 ± 26[b]	345 ± 90[b]	310 ± 58	154 ± 10[b]
	20.0	683 ± 47[b]	543 ± 150[b]	597 ± 108[b]	834 ± 162[b]	688 ± 98[b]

[a] Positive controls were 2-Aminofluorene (10 μg per plate, Sigma-Aldrich) for TA97, TA98 and TA100 strains, cyclophosphamide (CPA; 200 μg per plate, Sigma) for the TA1535 strain and 1,8-dihydroxyanthraquinone (50 μg per plate, Sigma–Aldrich) for the TA102 strain, respectively.
[b] $P < 0.05$, when compared to negative control.

activation, the number of revertant colonies for SMG-10 significantly increased at 0.032–20.0 μg per plate in TA97 and TA98, 4.0–20.0 μg per plate in TA100 and TA102, and 0.16–20.0 μg per plate in TA1535, when compared to that of negative control ($P < 0.05$). Moreover, the number of revertant colonies in all the above groups was two-fold higher than that in the negative control group, and there was also dose-dependence in the number of revertants induced by SMG-10. On the basis of available data, it was concluded that SMG-10 was mutagenic in all the tested strains with and without metabolic activation.

In the absence of metabolic activation, the number of revertant colonies induced by SMG-30 at all the concentrations was not significantly different from that in the negative

Table 3. Mammalian chromosome aberration test result (4h, with and without S9).

Group	Concentration (μg ml^{-1})	RCG (%)		Structural aberration (%)		Gap (%)		Polyploid (%)	
		−S9	+S9	−S9	+S9	−S9	+S9	−S9	+S9
Negative	0	100.0	100.0	0.5	2.0	0.5	0.0	0.0	0.5
Positive[a]		91.0	111.9	12.5[b]	19.5[b]	3.0	1.0	0.5	0.0
SEI-10	0.94	107.2	92.7	0.0	2.5	0.0	0.5	1.0	0.0
	1.88	101.7	101.3	1.0	0.0	0.0	0.5	0.5	0.5
	3.75	98.1	87.6	0.0	0.0	0.0	0.0	1.0	0.5
	7.5	88.6	84.9	0.0	0.0	0.0	0.5	0.5	0.0
	15.0	81.4	71.1	0.5	0.0	0.0	0.0	0.5	0.5
SMG-10	2.5	88.3	91.6	0.5	0.5	0.5	0.5	0.5	0.5
	5.0	82.1	84.5	0.5	0.5	0.5	0.5	0.5	0.5
	10.0	69.9	83.9	0.5	0.0	0.5	0.5	0.5	0.5
	20.0	73.8	74.0	0.0	0.0	0.5	0.5	1.0	1.5
SMG-30	2.5	88.3	88.2	1.0	0.0	0.5	0.5	0.0	0.5
	5.0	81.0	95.5	1.0	0.5	0.0	0.5	1.0	0.0
	10.0	76.9	87.0	0.0	0.5	1.0	0.5	0.5	0.0
	20.0	73.7	87.8	1.0	0.5	0.0	0.5	0.0	0.0

Note: a cell that had many aberrations was calculated as one cell showing aberrations. Structural chromosomal aberrations mainly included chromatid exchange and chromatid break. Gaps were recorded separately but not included in the total aberration frequency.
RCG: relative cell growth; polyploid (%): percent of polyploid metaphase cells, including endoreduplicated metaphase cells.
[a] Positive controls were CPA (25 μg ml^{-1}) with S9 mixture, MMC (0.25 μg ml^{-1}) without S9 mixture, respectively.
[b] $P<0.05$, when compared to negative control.

control group in any tested *S. typhimurium* strain. Therefore, SMG-30 was not mutagenic without metabolic activation. In the presence of metabolic activation, the number of revertant colonies induced by SMG-30 significantly increased at 0.16–20.0 μg per plate in TA97, 0.032–20.0 μg per plate in TA100, 20.0 μg per plate in TA102, and 4.0–20.0 μg per plate in TA98 and TA1535, when compared to that of negative control ($P<0.05$). Moreover, the number of revertant colonies generated was more than twice the number of revertant colonies in the negative control group. According to the evaluation criteria, the mutagenic activity of SMG-30 was judged to be positive in the presence of metabolic activation.

SEI did not cause the dose-dependent increase in the number of revertant colonies both in the absence and presence of metabolic activation. Although some increase or decrease in the number of revertants were found at a few concentrations in TA98 or TA100 tester strain, the number of revertant colonies generated is less than twice that in the negative control, and there was also no dose-response relationship. In addition, the decrease in the number of revertant colonies is not attributed to a cytotoxic effect of SEI-10, because the survival and the background of bacteria growth were similar to the negative control. In conclusion, there was no cytotoxicity for SEI-10 at the tested concentrations in all test strains, and its mutagenicity was found to be negative in all strains with or without S9 mix.

3.3. In vitro mammalian chromosome aberration test

The results were judged positive if reproducible and significant increases in the frequencies of structurally (excluding gaps) or numerically aberrant metaphases were observed at any concentration of IONPs with a dose-related response.

The results of chromosomal aberration test are shown in table 3 (4 h) and table 4 (24 h). No cytotoxicity was observed in CHL cells treated with SMG-10 and SMG-30. Cells treated with SEI-10 at 10 μg ml^{-1} exhibited growth inhibition. After the treatment of IONPs, the incidence of cells with structural chromosomal aberrations was less than 5% and that of polyploid cells was 0–2.0%, which are not significantly different from that in negative control, respectively. When compared to negative control, no increase in the incidence of either type of aberration was observed at all the tested concentrations of IONPs regardless of metabolic activation. From the results obtained under the conditions of this test, the *in vitro* clastogenic potential of all three IONPs (SMG-10, SMG-30 and SEI-10) was judged to be negative in the presence and absence of metabolic activation.

3.4. In vivo mammalian erythrocyte micronucleus test

The result was judged positive if a statistically significant increase in the frequency of MNPCE was observed in at least one dose level of IONPs, accompanied by statistically significant dose-response relationship.

Table 5 shows the results of micronucleus test. No abnormalities were observed at any dose of SMG-10, SMG-30 and SEI-10 after intravenous injection. The incidence of MNPCE in all the IONPs-treated groups was in the range of 1.583%–2.583%, which was not significantly different from that in the negative control group (2.000%), but the incidence in the positive control group (17.000%) was significantly higher than that in the negative control group ($P<0.05$). The incidence of PCE in the IONPs-treated groups (0.488%–0.579%) was not significantly different from that in the negative control group (0.535%). These results indicated that SMG-10, SMG-30 and SEI-10 did not cause *in vivo*

Table 4. Mammalian chromosome aberration test result (24 h, without S9).

Group	Concentration (μg ml^{-1})	RCG (%)	Structural aberration (%)	Gap (%)	Polyploid (%)
Negative	0	100.0	1.0	0.5	0.0
MMC	0.25	99.9	21.5[a]	4.5	0.0
SEI-10	0.63	93.7	0.5	0.0	0.0
	1.25	85.8	0.5	0.5	0.0
	2.5	81.9	1.5	0.0	1.5
	5.0	71.0	0.5	0.0	0.5
	10.0	50.1	1.5	0.5	0.5
SMG-10	2.5	81.9	1.5	0.0	0.0
	5.0	75.2	0.5	0.5	0.0
	10.0	77.0	0.5	0.5	0.0
	20.0	73.7	0.5	0.0	0.5
SMG-30	2.5	87.9	0.5	0.5	0.5
	5.0	79.1	0.5	1.0	0.5
	10.0	72.8	0.5	0.5	1.0
	20.0	75.7	0.5	0.5	0.5

Note: a cell that had many aberrations was calculated as one cell showing aberrations. Structural chromosomal aberrations mainly included chromatid exchange and chromatid break. Gaps were recorded separately but not included in the total aberration frequency.
RCG: relative cell growth; polyploid (%): percent of polyploid metaphase cells, including endoreduplicated metaphase cells.
[a] $P < 0.05$, when compared to negative control.

Table 5. Mouse bone marrow micronucleus test result ($n = 6$).

Treatment	Dose (mg kg^{-1})	MNPCE	PCE
Negative	0	2.000 ± 1.183	0.535 ± 0.110
CPA	40	17.000 ± 8.130[a]	0.508 ± 0.040
SEI-10	0.38	2.583 ± 0.665	0.515 ± 0.093
	0.75	2.250 ± 1.173	0.528 ± 0.090
	1.5	1.583 ± 0.917	0.539 ± 0.087
SMG-10	2.5	2.000 ± 1.844	0.488 ± 0.060
	5.0	1.583 ± 0.585	0.498 ± 0.082
	10.0	2.583 ± 1.744	0.493 ± 0.096
SMG-30	2.5	1.750 ± 1.037	0.528 ± 0.115
	5.0	2.750 ± 1.037	0.579 ± 0.075
	10.0	1.833 ± 1.291	0.545 ± 0.093

MNPCE: micronucleated polychromatic erythrocytes/2000 PCE; PCE: polychromatic erythrocytes/TE; TE: total erythrocytes.
[a] $P < 0.05$, when compared to negative control.

cytogenetic damage which resulted in the formation of micronuclei in bone marrow cells of mice.

4. Discussion

In the present study, a standard battery of assays, each known to have it particular genotoxic endpoints, were employed to evaluate the genotoxicity of IONPs with various size and surface coatings. For example, Ames test uses amino-acid requiring strains of *S. typhimurium* and *Escherichia coli* to detect point mutations, which involve substitution, addition or deletion of one or a few DNA base pairs [12]. The *in vitro* chromosome aberration test is used to detect structural chromosome aberrations in cultured mammalian cells [16]. The mammalian *in vivo* micronucleus test is used for the detection of damage induced by the test substance to the chromosomes or the mitotic apparatus of erythroblasts [18]. The results in our study demonstrated that IONPs with non-functional PEG coating exhibited concentration-dependent mutagenic activity in Ames test under the present experimental conditions. The data also indicated that IONPs with PEG coating may cause point mutations in *S. typhimurium* strains. These findings are consistent with some previous reports regarding the genotoxicity of iron nanoparticles. For example, Fe and Fe_2O_3 nanoparticles are known to be toxic and can cause significant DNA damage [19]. Gomaa *et al* [2] reported that the extent of DNA damage quantified by Comet assay and the mutagenicity study using Ames test were significantly correlated for the magnetite nanoparticles. Iron-platinum (FePt) nanoparticles tested were, with and without S9 mixture, weakly positive in the Ames test on *Salmonella* TA100 strain [20].

Our studies also indicated that larger IONPs with PEG coating (SMG-30) did not have mutagenic activity in the absence of metabolic activation, but presented mutagenic activity in the presence of metabolic activation, suggesting that the genotoxic metabolites of SMG-30 may be generated by adding metabolic activation. Kumar *et al* [21] also reported that ZnO nanoparticles exhibited mutagenic potential in the presence of S9 mix. This could either be due to the formation of micelles of nanoparticles in presence of metabolic activation [22] or the protein present in the S9 mix which may coat NPs and thus facilitate entry into the cells [23].

The toxicity of IONPs is affected by their composition, much like the parent bulk materials. However, additional physico-chemical properties such as particle size play a crucial role in determining the toxicity of nanomaterials [24]. As shown in the present Ames study, IONPs demonstrated the size-dependent mutagenic activity. Smaller IONPs with PEG coating (SMG-10) showed stronger mutagenic potential than

larger IONPs with the same coating (SMG-30). Other groups also reported that particle size dramatically affected the toxicity of nanoparticles. Song *et al* [25] investigated the human toxicity of polyacrylate nanoparticles (between 40 and 250 nm in size) prepared from polymerization of unsaturated monomers, such as methyl methacrylate, methacrylic amide or cyanoacrylates [26]. The toxicity of the larger cyanoacrylate nanoparticles was correlated with chemical properties and molecule chain length and was independent of particle size [27]. However, smaller polyacrylate nanoparticles produced toxic effects independently of chemistry [25].

Particle size and surface area are crucial material characteristics from a toxicological point of view, as interactions between nanomaterials and biological organisms typically take place at the surface of the nanoparticles. As the particles' size decreases, the surface area exponentially increases and a greater proportion of the particles' atoms or molecules will be displayed on the surface rather than within the bulk of the material [24]. Since it is known that the endocytic mode, uptake and efficiency of particles in the cells are dependent on size of material [28–31], particle size plays a key role in physiological response, distribution, and elimination of materials [32, 33]. Kumar *et al* [21] reported that the small nanoparticles can enter the bacterial cells and may interact with the cellular macromolecules inducing weak mutagenic potential in Ames test of ZnO and TiO_2 nanoparticles. Guan *et al* [34] also observed the DNA-damaging effects of ZnO NPs (about 50 nm, TEM) in L02 and HEK293 cells, which was attributed to lipid peroxidation and oxidative stress. In our study the stronger mutagenic effect of SMG-10 compared to SMG-30 might be explained by its better penetration into the cell wall of bacterial cells due to its smaller particle size.

Besides particle size, surface coating was also demonstrated to dramatically affect the genotoxicity of IONPs in our study. IONPs with the same particle size, but with different surface coating (neutral PEG coating, SMG-10; or positively charged PEI coating, SEI-10) showed completely different toxicity characteristic. SEI-10 was not genotoxic in the standard battery of tests. However, it was cytotoxic against CHL cells and toxic in NIH mice via intravenous injection in our laboratory conditions. It was previously reported that cationic polymers such as PEI and polylysine (PLL) may exert their cytotoxicity by inducing necrosis or apoptosis through mitochondria mediated pathways [35]. In addition, preliminary data in our laboratory demonstrated that SEI-10 had hemolytic activity (data not published), which might partially contribute the animal death induced by the high dose of SEI-10 in this study. On the contrary, IONPs with PEG coating and the same particle size (SMG-10) exhibited dose-dependent mutagenic activity in all of the *S. typhimurium* strains (TA97, TA98, TA100, TA102 and TA1535) with and without metabolic activation. Our observation is in agreement with a recent report from Klien K and Gondić-Cvar J [36], which demonstrated that nanoparticulate coatings seem to have a relevant impact on genotoxicity, as they not only alter the particles' surface charge, but also change their agglomeration status by which they gain total surface area. Surface coatings of nanoparticles can modify their surface charge or surface composition, which has important impact on the intracellular distribution and the production of ROS that cause further toxicity [24]. For example, multi-wall carbon nanotubes (MWCNT) were shown to evade the reticuloendothelial system (RES) when their surface is coated with ammonium and chelator functional groups [37] but were taken up when coated with taurine [38]. Normally, magnetic nanoparticles are surrounded by coatings to prevent the presence of free iron oxide, but the coating may be metabolized after some time [39]. It has been shown that dextran-magnetite (Fe_3O_4) nanoparticles cause cell death and reduced proliferation similar to uncoated iron oxide particles, which was attributed to the breakdown of the dextran shell exposing the cellular components to chains or aggregates of IONPs [40]. Xie *et al* [41] also showed that coating PEG on monodisperse Fe_3O_4 nanoparticles produced negligible aggregation in cell culture conditions and reduced non-specific uptake by macrophage cells. Although PEGylation may reduce the potential of harmful biological interactions, Cho *et al* [42] found that 13 nm sized Au nanoparticles coated with PEG 5000 induce acute inflammation and apoptosis in the mouse liver. These nanoparticles were found to accumulate in the liver and spleen for up to seven days after injection and to have a long blood circulation time of about 30 h. A relatively high concentration of PEG on the nanoparticles surface alone does not lead to a lower NP uptake, but rather the spatial configurational freedom of PEG chains on the particle surface plays a determinant role [43]. Polysaccharide-coated Ag nanoparticles increased the expression of tumor suppressor proteins but uncoated Ag nanoparticles did not [44, 45]. The opposite effect was seen with cobalt-based nanoparticles. While silica-coated cobalt ferrite nanoparticles were non-genotoxic, uncoated cobalt ferrite nanoparticles significantly increased the expression of genes associated with DNA damage and repair [46]. As mentioned above, the increased genotoxic effect of polysaccharide-coated nanoparticles might be due to the inhibition of particle agglomeration [44]. Coatings based on silica might prevent the oxidatively damaging capability of cobalt ferrite nanoparticles. Uncoated cobalt ferrite nanoparticles might release metal ions due to direct interaction with cell membranes, which in turn could result in oxidative stress and consequent DNA damage. These results indicate that the derivatization of iron oxide plays an important role in the internalization efficiency and cytotoxicity [1].

Another important factor to determine the genotoxicity of nanoparticles is the electrical charge of the particle surface [36]. Sharifi *et al* [24] reported that surface charge also plays a role in toxicity, as it influences the adsorption of ions and biomolecules that may change organism or cellular responses toward particles. In addition, surface charge is a major determinant of colloidal behavior, which influences the organism response by changing the shape and size of nanoparticles through aggregate or agglomerate formation [47]. In general, it is believed that cationic surfaces are more toxic than anionic surfaces, and cationic surfaces are more likely to induce hemolysis and platelet aggregation, whereas neutral surfaces are the most biocompatible [48]. This may be due to

the affinity of cationic particles to the negative phospholipid head groups or protein domains on cell membranes. In addition surface charge influences plasma protein binding, which in turn affects the *in vivo* organ distribution and clearance of nanoparticles from the circulation. For example, Saxena *et al* [49] showed that acid-functionalized SWCNTs caused markedly significant *in vivo* toxicity compared to pristine SWCNTs. This higher toxicity could result either from a possible greater bioavailability of well dispersed AF-SWCNT preparations, or from the high negative charge on AF-SWCNTs, or both. Pietroiusti *et al* [50] found that AF-SWCNTs had a marked embryotoxic effect compared to pristine SWCNTs in pregnant mice models. Similarly, increased toxicity was attributed to a higher percentage of monodispersed SWCNTs in acid functionalized SWCNTs and higher negative charge and hydrophilicity. There is report that the charge of surface coatings may affect the toxicity of QD nanoparticles. Kim *et al* [51] investigated QDs coated with the negatively charged serum protein albumin. They observed a higher liver uptake (99%) and faster blood clearance relative to the QDs without albumin (40%). Geys *et al* [52] investigated the *in vivo* toxicity of positively charged (amine-QDs) and negatively charged (carboxyl-QDs) quantum dots after intravenous injection in mice. They found that the carboxyl-QDs caused more pulmonary vascular thrombosis than amine-QDs at high doses. The presence of fibrin fibers in the thrombi suggests that negatively charged QDs activate the coagulation cascade via contact activation. Hoshino *et al* [47] studied a series of QDs with different surface coatings (carboxyl, hydroxyl, amine or their combinations). They found that the highly negatively charged QDs with carboxyl groups induced DNA damage after 2 h, while the other types did not induce significant cellular damage. Bhattacharjee *et al* [53] showed positively charged Si nanoparticles (Si-NP-NH_2) proved to be more cytotoxic than neutral Si (NP-N_3) in terms of reduced mitochondrial metabolic activity and phagocytosis, while negatively charged Si (Si-NP-COOH) had very little or no cytotoxicity. Heiden *et al* [54] and Malik *et al* [55] reported that surface charge also impacts the toxicity of dendrimers. Positively charged PAMAM dendrimers (G4) showed time-dependent toxicity toward zebrafish embryos; however, anionic PAMAM dendrimers had no toxicity. Similar results have been reported when anionic PAMAM dendrimers were administrated to mice. Nanoparticle surface charge also has been observed to alter blood-brain barrier integrity and permeability [56]. It is suggested that high concentrations of anionic nanoparticles and cationic nanoparticles are able to disrupt the integrity of the blood brain barrier [24]. Particle surface charge can also impact transdermal permeation of charged nanoparticles. It was found that after dermal administration, negatively charged nanoparticles of about 50 and 500 nm permeated the skin, while positively charged and neutral particles of all sizes did not [56]. The above analysis may provide some important clues to explain that neutral IONPs with PEG coating (SMG-10) and positively charged IONPs with PEI surface (SEI-10) showed completely different toxicity characteristics.

It can be concluded that the toxicity of IONPs can be influenced by particles size, surface coating, and surface charge. The research of Klien K and Gondić-Cvar J [36] also showed that the currently available animal studies may suggest differing genotoxic mechanisms depending on the duration of exposure. At present, our study only limited to short-term genotoxicity testing. Next, *in vitro* and *in vivo* genotoxicity testing will have to be conducted for longer periods to observe if there are long-term effects of IONPs such as tumor formation and carcinogenesis. Treatment intervals will have to go beyond days to weeks or even months in animal studies. It will also be useful to look at the clearance of IONPs from the body and to study if there is a preference for accumulation in certain organs and any effect from biopersistence of such IONPs [57].

In conclusion, IONPs with PEI coating had no genotoxic effect in the battery of standardized tests, whereas IONPs with PEG coating had size-dependent mutagenic activity in Ames test, although no other types of mutations such as chromosome aberration were found in other tests. These data indicate that physical and chemical properties of IONPs are important for assessing the mutagenic and transformation activity leading to their genotoxicity. Results of this study extend the knowledge on the safety of iron oxide nanoparticles with different coatings in view of their possible medical applications, such as in diagnosis, therapy and drug targeted delivery.

Acknowledgment

This work was supported by National Natural Science Foundation of China (81101143), and the Fundamental Research Funds for the Central Universities (2082604174150).

Conflict of interest

The authors declare that there are no conflicts of interest.

References

[1] Singh N, Manshian B, Jenkins G J, Griffiths S M, Williams P M, Maffeis T G, Wright C J and Doak S H 2009 NanoGenotoxicology: the DNA damaging potential of engineered nanomaterials *Biomaterials* **30** 3891–914
[2] Gomaa I O, Kader M H, Salah T A and Heikal O A 2013 Evaluation of *in vitro* mutagenicity and genotoxicity of magnetite Nanoparticles *Drug Discov. Ther.* **7** 116–23
[3] Naqvi S, Samim M, Abdin M, Ahmed F J, Maitra A, Prashant C and Dinda A K 2010 Concentration-dependent toxicity of iron oxide nanoparticles mediated by increased oxidative stress *Int. J. Nanomedicine* **5** 983–9
[4] Szalay B, Tátrai E, Nyírő G, Vezér T and Dura G 2012 Potential toxic effects of iron oxide nanoparticles in *in vivo* and *in vitro* experiments *J. Appl. Toxicol.* **32** 446–53
[5] Sahu S C and Casciano D A 2009 *Nanotoxicity: From In Vivo and In Vitro Models to Health Risks* (UK: Wiley)

[6] Sadiq R, Khan Q M, Mobeen A and Hashmat A J 2014 *In vitro* toxicological assessment of iron oxide, aluminium oxide and copper nanoparticles in prokaryotic and eukaryotic cell types *Drug Chem. Toxicol.* [Epub ahead of print] doi:10.3109/01480545.2014.919584

[7] Woodruff R S, Li Y, Yan J, Bishop M, Jones M Y, Watanabe F, Biris A S, Rice P, Zhou T and Chen T 2012 Genotoxicity evaluation of titanium dioxide nanoparticles using the Ames test and Comet assay *J. Appl. Toxicol.* **32** 934–43

[8] Alexis F, Pridgen E, Molnar L K and Farokhzad O C 2008 Factors affecting the clearance and biodistribution of polymeric nanoparticles *Mol. Pharm.* **5** 505–15

[9] Xiao K, Li Y, Luo J, Lee J S, Xiao W, Gonik A M, Agarwal R G and Lam K S 2011 The effect of surface charge on *in vivo* biodistribution of PEG-oligocholic acid based micellar nanoparticles *Biomaterials* **32** 3435–46

[10] Xiao K, Luo J, Fowler W L, Li Y, Lee J S, Xing L, Cheng R H, Wang L and Lam K S 2009 A self-assembling nanoparticle for paclitaxel delivery in ovarian cancer *Biomaterials* **30** 6006–16

[11] Elliott B M, Combes R D, Elcombe C R, Gatehouse D G, Gibson G G, Mackay J M and Wolf R C 1992 Alternatives to aroclor 1254-induced S9 in *in vitro* genotoxicity assays *Mutagenesis* **7** 175–7

[12] OECD (Organization for Economic Cooperation and Development) 1997 Guideline 471 *Guideline for the Testing of Chemicals: Bacteria Reverse Mutation Test* www.oecd.org/chemicalsafety/risk-assessment/1948418.pdf (Adopted 21st July, 1997)

[13] Ames B N, Durston W E, Yamasaki E and Lee F D 1973 Carcinogens are mutagens: a simple test system combining liver homogenates for activation and bacteria for detection *Proc. Natl. Acad. Sci. USA* **70** 2281–5

[14] Maron D M and Ames B N 1983 Revised methods for the Salmonella mutagenicity test *Mutat. Res.* **113** 173–215

[15] Ames B N, McCann J and Yamasaki E 1975 Methods for detecting carcinogens and mutagens with the Salmonella/mammalian-microsome mutagenicity test *Mutat. Res.* **31** 347–64

[16] OECD (Organization for Economic Cooperation and Development) 1997 Guideline 473 *Guideline for the Testing of Chemicals: In vitro Mammalian Chromosome Aberration Test* www.oecd.org/chemicalsafety/risk-assessment/1948442.pdf (Adopted 21st July, 1997)

[17] Maenosono S, Yoshida R and Saita S 2009 Evaluation of genotoxicity of amine-terminated water-dispersible FePt nanoparticles in the Ames test and *in vitro* chromosomal aberration test *J. Toxicol. Sci.* **34** 349–54

[18] OECD (Organization for Economic Cooperation and Development) 1997 Guideline 474 *Guideline for the Testing of Chemicals: Mammalian Erythrocyte Micronucleus Test* www.oecd.org/chemicalsafety/risk-assessment/1948442.pdf (Adopted 21st July, 1997)

[19] Trouiller B, Reliene R, Westbrook A, Solaimani P and Schiestl R H 2009 Titanium dioxide nanoparticles induce DNA damage and genetic instability *in vivo* in mice *Cancer Res.* **69** 8784–9

[20] Maenosono S, Suzuki T and Saita S 2007 Mutagenicity of water-soluble FePt nanoparticles in Ames test *J. Toxicol. Sci.* **32** 575–9

[21] Kumar A, Pandey A K, Singh S S, Shanker R and Dhawan A 2011 Cellular uptake and mutagenic potential of metal oxide nanoparticles in bacterial cells *Chemosphere* **83** 1124–32

[22] Sereemaspun A, Hongpiticharoen P, Rojanathanes R, Maneewattanapinyo P, Ekgasit S and Warisnoicharoen W 2008 Inhibition of human cytochrome P450 enzymes by metallic nanoparticles: a preliminary to nanogenomics *Int. J. Pharmacol.* **4** 492–5

[23] Romberg B, Hennink W E and Storm G 2008 Sheddable coatings for long-circulating nanoparticles *Pharm. Res.* **25** 55–71

[24] Sharifi S, Behzadi S, Laurent S, Forrest M L, Stroeve P and Mahmoudi M 2012 Toxicity of nanomaterials *Chem. Soc. Rev.* **41** 2323–43

[25] Song Y, Li X and Du X 2009 Exposure to nanoparticles is related to pleural effusion, pulmonary fibrosis and granuloma *Eur. Respir. J.* **34** 559–67

[26] Kreuter J 2007 Nanoparticles–a historical perspective *Int. J. Pharm.* **331** 1–10

[27] Lherm C, Müller R H, Puisieux F and Couvreur P 1992 Alkylcyanoacrylate drug carriers: II. Cytotoxicity of cyanoacrylate nanoparticles with different alkyl chain length *Int. J. Pharm* **84** 13–22

[28] Aillon K L, Xie Y, El-Gendy N, Berkland C J and Forrest M L 2009 Effects of nanomaterial physicochemical properties on *in vivo* toxicity *Adv. Drug Delivery Rev.* **61** 457–66

[29] Lanone S and Boczkowski J 2006 Biomedical applications and potential health risks of nanomaterials: molecular mechanisms *Curr. Mol. Med.* **6** 651–63

[30] Nel A, Xia T, Mädler L and Li N 2006 Toxic potential of materials at the nanolevel *Science* **311** 622–7

[31] Rejman J, Oberle V, Zuhorn I S and Hoekstra D 2004 Size-dependent internalization of particles via the pathways of clathrin- and caveolae-mediated endocytosis *Biochem. J.* **377** 159–69

[32] Powers K W, Brown S C, Krishna V B, Wasdo S C, Moudgil B M and Roberts S M 2006 Research strategies for safety evaluation of nanomaterials. VI. Characterization of nanoscale particles for toxicological evaluation *Toxicol. Sci.* **90** 296–303

[33] Powers K W, Palazuelos M, Moudgil B M and Roberts S M 2007 Characterization of the size, shape, and state of dispersion of nanoparticles for toxicological studies *Nanotoxicology* **1** 42–51

[34] Guan R, Kang T, Lu F, Zhang Z, Shen H and Liu M 2012 Cytotoxicity, oxidative stress, and genotoxicity in human hepatocyte and embryonic kidney cells exposed to ZnO nanoparticles *Nanoscale Res. Lett.* **7** 602

[35] Hunter A C and Moghimi S M 2010 Cationic carriers of genetic material and cell death: a mitochondrial tale *Biochim. Biophys. Acta* **1797** 1203–9

[36] Klien K and Gondić-Cvar J 2012 Genotoxicity of metal nanoparticles: focus on *in vivo* studies *Arh Hig Rada Toksikol* **63** 133–45

[37] Singh R, Pantarotto D, Lacerda L, Pastorin G, Klumpp C, Prato M, Bianco A and Kostarelos K 2006 Tissue biodistribution and blood clearance rates of intravenously administered carbon nanotube radiotracers *Proc. Natl. Acad. Sci. USA* **103** 3357–62

[38] Deng X, Jia G, Wang H, Sun H, Wang X, Yang S, Wang T and Liu Y 2007 Translocation and fate of multi-walled carbon nanotubes *In Vivo Carbon* **45** 1419–24

[39] Schulze E, Ferrucci J T Jr, Poss K, Lapointe L, Bogdanova A and Weissleder R 1995 Cellular uptake and trafficking of a prototypical magnetic iron oxide label *in vitro Invest. Radiol.* **30** 604–10

[40] Berry C C, Wells S, Charles S and Curtis A S 2003 Dextran and albumin derivatised iron oxide nanoparticles: influence on fibroblasts *in vitro Biomaterials* **24** 4551–7

[41] Xie J, Xu C, Kohler N, Hou Y and Sun S 2007 Controlled PEGylation of monodisperse Fe_3O_4 nanoparticles for reduced non-specific uptake by macrophage cells *Adv. Mater.* **19** 3163–6

[42] Cho W S, Cho M, Jeong J, Choi M, Cho H Y, Han B S, Kim S H, Kim H O, Lim Y T, Chung B H and Jeong J 2009 Acute toxicity and pharmacokinetics of 13 nm-sized PEG-coated gold nanoparticles *Toxicol. Appl. Pharmacol.* **236** 16–24

[43] Hu Y, Xie J, Tong Y W and Wang C H 2007 Effect of PEG conformation and particle size on the cellular uptake efficiency of nanoparticles with the HepG2 cells *J. Control. Release* **118** 7–17

[44] Ahamed M, Karns M, Goodson M, Rowe J, Hussain S M, Schlager J J and Hong Y 2008 DNA damage response to different surface chemistry of silver nanoparticles in mammalian cells *Toxicol. Appl. Pharmacol.* **233** 404–10

[45] Ahamed M, Posgai R, Gorey T J, Nielsen M, Hussain S M and Rowe J J 2010 Silver nanoparticles induced heat shock protein 70, oxidative stress and apoptosis in *Drosophila melanogaster Toxicol. Appl. Pharmacol.* **242** 263–9

[46] Hwang do W, Lee D S and Kim S 2012 Gene expression profiles for genotoxic effects of silica-free and silica-coated cobalt ferrite nanoparticles *J. Nucl. Med.* **53** 106–12

[47] Hoshino A, Fujioka K, Oku T, Suga M, Sasaki Y F, Ohta T, Yasuhara M, Suzuki K and Yamamoto K 2004 Physicochemical properties and cellular toxicity of nanocrystal quantum dots depend on their surface modification *Nano. Lett.* **4** 2163–9

[48] Goodman C M, McCusker C D, Yilmaz T and Rotello V M 2004 Toxicity of gold nanoparticles functionalized with cationic and anionic side chains *Bioconjug. Chem.* **15** 897–900

[49] Saxena R K, Williams W, Mcgee J K, Daniels M J, Boykin E and Ian Gilmour M 2007 Enhanced *in vitro* and *in vivo* toxicity of poly-dispersed acid-functionalized single-wall carbon nanotubes *Nanotoxicology* **1** 291–300

[50] Pietroiusti A, Massimiani M, Fenoglio I, Colonna M, Valentini F, Palleschi G, Camaioni A, Magrini A, Siracusa G, Bergamaschi A, Sgambato A and Campagnolo L 2011 Low doses of pristine and oxidized single-wall carbon nanotubes affect mammalian embryonic development *ACS Nano* **5** 4624–33

[51] Kim S, Fisher B, Eisler H J and Bawendi M 2003 Type-II quantum dots: CdTe/CdSe(core/shell) and CdSe/ZnTe (core/shell) heterostructures *J. Am. Chem. Soc.* **125** 11466–7

[52] Geys J, Nemmar A, Verbeken E, Smolders E, Ratoi M, Hoylaerts M F, Nemery B and Hoet P H 2008 Acute toxicity and prothrombotic effects of quantum dots: impact of surface charge *Environ. Health Perspect.* **116** 1607–13

[53] Bhattacharjee S, de Haan L H, Evers N M, Jiang X, Marcelis A T, Zuilhof H, Rietjens I M and Alink G M 2010 Role of surface charge and oxidative stress in cytotoxicity of organic monolayer-coated silicon nanoparticles towards macrophage NR8383 cells *Part. Fibre Toxicol.* **7** 25

[54] Heiden T C, Dengler E, Kao W J, Heideman W and Peterson R E 2007 Developmental toxicity of low generation PAMAM dendrimers in zebrafish *Toxicol. Appl. Pharmacol.* **225** 70–9

[55] Malik N, Evagorou E G and Duncan R 1999 Dendrimer-platinate: a novel approach to cancer chemotherapy *Anticancer Drugs* **10** 767–76

[56] Lockman P R, Koziara J M, Mumper R J and Allen D D 2004 Nanoparticle surface charges alter blood-brain barrier integrity and permeability *J. Drug Target* **12** 635–41

[57] Ng C T, Li J J, Bay B H and Yung L Y 2010 Current studies into the genotoxic effects of nanomaterials *J. Nucleic Acids* 947859